

1 **Zein based-Nanoparticles Improve the Oral Bioavailability of Resveratrol**  
2 **and its Anti-inflammatory Effects in a Mouse model of Endotoxic Shock**

3

4 **Authors**

5 Rebeca Penalva <sup>a</sup>, Irene Esparza <sup>a</sup>, Eneko Larraneta <sup>a</sup>, Carlos J. González-Navarro <sup>c</sup>,  
6 Carlos Gamazo <sup>b</sup>, Juan M. Irache <sup>a</sup>

7

8 **Affiliation**

9 <sup>a</sup> Department of Pharmacy and Pharmaceutical Technology, University of Navarra,  
10 31008 - Pamplona, Spain.

11 <sup>b</sup> Department of Microbiology. University of Navarra, 31008 - Pamplona, Spain.

12 <sup>c</sup> Centre for Nutrition Research, University of Navarra, 31080 - Pamplona, Spain.

13

14 **Corresponding author:**

15 Prof. Juan M. Irache  
16 Dep. Pharmacy and Pharmaceutical Technology  
17 University of Navarra  
18 C/ Irunlarrea, 1  
19 31080 – Pamplona  
20 Spain  
21 Phone: +34948425600  
22 Fax: +34948425619  
23 E-mail: jmirache@unav.es

24

25 **Running title:** Zein nanoparticles improve bioavailability and antiinflammatory  
26 effect of resveratrol

27 **Abstract**

28 Resveratrol offers pleiotropic health beneficial effects including its reported capability to  
29 inhibit lipopolysaccharide (LPS) induced cytokine production. The aim of this work was  
30 to prepare, characterize and evaluate a resveratrol nanoparticulate formulation based  
31 on zein. For this purpose the oral bioavailability of the encapsulated polyphenol as well  
32 as its anti-inflammatory effect in a mouse model of endotoxic shock were studied.

33 Resveratrol-loaded nanoparticles displayed sizes around 300 nm with a negative zeta  
34 potential (- 51 mV) and a polyphenol loading close to 80 µg/mg. In vitro, the release of  
35 resveratrol from the nanoparticles was found to be pH-independent and adjusted well  
36 to the Peppas-Salin kinetic model, suggesting a mechanism based on the combination  
37 between diffusion and erosion of the nanoparticle matrix. Pharmacokinetic studies  
38 demonstrated that zein-based nanoparticles provided high and prolonged plasma  
39 levels of the polyphenol for at least 48 h. The oral bioavailability of resveratrol when  
40 administered in these nanoparticles increased up to 50% (20-fold higher than for the  
41 control solution of the polyphenol). Furthermore, nanoparticles administered daily for 7  
42 days at 15 mg/kg, were able to diminish the endotoxic symptoms induced in mouse by  
43 the ip administration of LPS (i.e. hypothermia, piloerection and stillness). In addition,  
44 serum TNF-α levels were slightly lower (about 15%) of those observed for the control.

45

46 **Key words**

47 Resveratrol, zein, nanoparticles, bioavailability, anti-inflammatory.

48

49

50 **Abbreviations**

51 Rsv: resveratrol

52 SIRT1: sirtuin 1

53 LPS: lipopolysaccharide from Salmonella enterica serovar. Minnesota

54 Rsv-NP-Z: resveratrol-loaded zein nanoparticles

55 NP-Z: empty zein nanoparticles

56 Rsv-sol: resveratrol solution in a PEG 400: water mixture

57 Rsv-susp: suspension of resveratrol in purified water

58 PCS: photon correlation spectroscopy

59 SEM: Scanning electron microscopy

60 EE: encapsulation efficiency

61 iv: intravenous

62  $C_{max}$ : maximal serum concentration

63  $T_{max}$ : time in which  $C_{max}$  is reached

64 AUC: area under the concentration-time curve from time 0 to last time

65 MRT: mean residence time

66 Cl: clearance

67 V: volume of distribution

68  $t_{1/2}$ : half-life in the terminal phase

69 Fr: relative bioavailability

70 FRD: fraction of resveratrol dissolved

71 FRA: fraction of resveratrol absorbed

72 ip: intraperitoneal

73 PGE2: prostaglandin E2

74 PDI: polydispersity index

75

## 76 **Introduction**

77 Resveratrol (Rsv) (3,5,4'-trihydroxy-trans-stilbene), is a polyphenol molecule that was  
78 identified from the dried roots of *Polygonum cuspidatum*, a plant used in traditional  
79 Chinese and Japanese medicine <sup>1</sup>. Resveratrol has been classified as a phytoalexin as  
80 it is synthesized in spermatophytes in response to injury, UV irradiation and fungal  
81 attack <sup>2</sup>. It is naturally found in a wide variety of plant species, vegetables, fruits and  
82 food products such as peanuts, grape skin, plums or red wine <sup>2</sup>.

83 Resveratrol offers pleiotropic health beneficial effects, including antioxidant and anti-  
84 aging effects <sup>3</sup>, cardioprotective <sup>4</sup>, anticancer <sup>1</sup>, neuroprotective <sup>5</sup> and HIV/AIDS  
85 activities <sup>6</sup>.

86 In the last years, it has been demonstrated the preventive effect of resveratrol against  
87 diabetes. Resveratrol would normalize hyperglycaemia and, in animals with  
88 hyperinsulinemia, it would reduce blood insulin <sup>7</sup>. Similarly, resveratrol was reported to  
89 reduce body weight and adiposity in obese recipients <sup>8</sup>. These actions would involve  
90 the activation of sirtuin 1 (SIRT1) that inhibits inflammatory pathways in macrophages  
91 and modulates insulin sensitivity <sup>9</sup>. Furthermore, different studies have shown that  
92 resveratrol is capable of inhibiting lipopolysaccharide (LPS) induced cytokine  
93 production <sup>10</sup>. This effect, via modulation of NF- $\kappa$ B, would decrease the production and  
94 gene expression of IL1 and TNF- $\alpha$ , important endogenous pyrogens <sup>11</sup>.

95 In spite of these potential health benefits, the use of resveratrol is limited due to its high  
96 lipophilicity, short biological half-life, and chemical instability. In addition, when  
97 resveratrol is orally administered, only trace amounts of the unchanged polyphenol can  
98 be detected in plasma <sup>12</sup>. This low bioavailability is due to the polyphenol  
99 biotransformation by UDP-glucuronosyltransferase and sulphotransferases that  
100 produces resveratrol-3'-glucuronide and the sulphate derivative, respectively <sup>2</sup>. In rats,  
101 the main metabolite of resveratrol is the glucuronide conjugate <sup>13</sup>, whereas, in humans,  
102 both the glucuronide and the sulphate derivatives have been described <sup>14</sup>. These  
103 metabolites have a longer plasma half-life, however, their efficacy are unknown <sup>1</sup>.

104 Renal excretion is the major route of elimination of the polyphenol and its derivatives  
105 <sup>2,15</sup>.

106 In order to solve these drawbacks different strategies have been pursued including its  
107 encapsulation in different oral delivery systems such as, among others, self-nano  
108 emulsifying drug delivery systems <sup>16</sup>, solid lipid nanoparticles <sup>17</sup> and polymeric  
109 nanoparticles <sup>18</sup>.

110 An alternative approach might be the use of zein nanoparticles. Zein is the major  
111 storage protein of maize and comprises approx. 45-50% of the total protein content in  
112 corn <sup>19</sup>. Since zein is a natural protein, it is actually a heterogeneous mixture of  
113 different peptides than can be divided in four main fractions: i)  $\alpha$ -zein (75-85% of total  
114 protein) with two main MW of 21-25 kDa and 10kDa, ii)  $\beta$ -zein (10-15%) of a MW of  
115 17-18 kDa, iii)  $\delta$ -zein, a minor fraction of 10kDa and vi)  $\gamma$ -zein (5-10%) with a MW of 27  
116 kDa <sup>19,20</sup>. Zein is an amphiphilic protein, possessing high percentages of hydrophobic  
117 amino acids such as leucine (20%), proline (10%) and alanine (10%) <sup>19,20</sup>. Due to this  
118 amino acid composition, zein is insoluble in water and, thus, the resulting devices (e.g.  
119 films, nanoparticles) display an hydrophobic character with interesting properties to  
120 control the release of the loaded compound <sup>20,21</sup>. In addition, as for other nanocarriers  
121 from protein origin, they are biodegradable and can accommodate a great variety of  
122 compounds in a non-specific way <sup>22</sup>.

123 Therefore, the aim of this work was to prepare, characterize and evaluate a resveratrol  
124 nanoparticulate formulation based on zein and to study its oral bioavailability and anti-  
125 inflammatory effect in a mouse model of induced endotoxic shock.

126

## 127 **Material and Methods**

### 128 **Chemicals**

129 Zein, resveratrol, lysine, mannitol, sodium ascorbate, poly(ethylene glycol) 400 (PEG  
130 400) and Tween 20 were purchased from Sigma-Aldrich (Germany). Resveratrol-3-O-

131 D-glucuronide (Rsv-O-glu) was from @rtMolecule (Poitiers, France). Ethanol,  
132 methanol, acetic acid and acetonitrile HPLC grade were obtained from Merck  
133 (Darmstadt, Germany). Lipopolysaccharide from *Salmonella enterica* serovar.  
134 Minnesota (LPS) was purchased from Sigma®, (St. Louis, USA). Deionised reagent  
135 water (18.2 MO resistivity) was prepared using a water purification system (Wasserlab,  
136 Spain). All reagents and chemicals used were of analytical grade.

### 137 **Preparation of resveratrol-loaded nanoparticles (Rsv-NP-Z)**

138 Nanoparticles were prepared by a desolvation method followed by an ultrafiltration  
139 purification step and subsequent drying in a spray-drier apparatus. Briefly, 600 mg zein  
140 and 100 mg lysine were dissolved in 60 mL of an ethanol:water mixture (65% ethanol  
141 by vol.). In parallel, 100 mg resveratrol were dissolved in 10 mL ethanol and 6 mL of  
142 this solution were transferred to the zein solution. In addition, 6 mg sodium ascorbate  
143 were added to minimise the oxidation of the polyphenol. The mixture was magnetically  
144 stirred in the dark for 10 min at room temperature. Nanoparticles were obtained by the  
145 continuous addition of 60 mL of purified water. The suspension was purified and  
146 concentrated by ultrafiltration using a 50 kDa pore size polysulfone membrane  
147 cartridge (Medica SPA, Italy). Then, 15 mL of purified water containing 1.2 g mannitol  
148 were added to the resulting suspension of nanoparticles to prevent aggregation and  
149 irreversible interactions among nanoparticles during the drying process. Finally the  
150 suspension was dried in a Büchi Mini Spray Drier B-290 apparatus (Büchi Labortechnik  
151 AG, Switzerland) under the following experimental conditions: (i) inlet temperature: 90  
152 °C, (ii) outlet temperature: 45-50 °C, (iii) air pressure: 4-6 bar, (iv) pumping rate: 5  
153 mL/min, (v) aspirator: 100% and (vi) air flow: 400-500 L/h.

154 Control formulations (NP-Z) were prepared as described above but in absence of  
155 resveratrol.

### 156 **Preparation of resveratrol conventional formulations**

157 Two different formulations of resveratrol were also prepared. The first one, a solution of  
158 the polyphenol in a mixture of PEG400 and water (1:1 by vol.) was preparing dissolving

159 37.5 mg of resveratrol in 5 mL of PEG400 under magnetic stirring. Then 5 mL of  
160 purified water were added and the final mixture was agitated in the dark for 10 min.  
161 This formulation was named Rsv-sol.

162 The second one was an extemporary suspension of resveratrol in purified water (Rsv-  
163 susp). Briefly, 37.5 mg of resveratrol were dispersed in 10 mL of purified water under  
164 magnetic agitation for 10 min. The size of the resulting suspension was  $21.4 \pm 9.2 \mu\text{m}$ .  
165 The suspension was used after inspection for absence of aggregates.

## 166 **Characterization of nanoparticles**

### 167 **Size, zeta potential and morphology**

168 The mean hydrodynamic diameter and the zeta potential of nanoparticles were  
169 determined by photon correlation spectroscopy (PCS) and electrophoretic laser  
170 Doppler anemometry, respectively, using a Zetamaster analyzer system (Malvern  
171 Instruments Ltd., Worcestershire, UK). The diameter of the nanoparticles was  
172 determined after dispersion in ultrapure water (1:10) and measured at 25 °C with a  
173 scattering angle of 90 °C. The zeta potential was measured after dispersion of the dried  
174 nanoparticles in 1 mM KCl solution.

175 The morphology of the nanoparticles was studied using a field emission scanning  
176 electron microscopy (SEM) in a Zeiss DSM940 digital scanning electron microscope  
177 (Oberkochen, Germany) coupled with a digital image system (Point Electronic GmbH,  
178 Germany). The yield of the process was calculated by gravimetry as described  
179 previously<sup>22</sup>.

### 180 **Resveratrol analysis**

181 The amount of resveratrol loaded into the nanoparticles was quantified by HPLC-UV  
182 following an analytical method previously described<sup>23</sup> with minor modifications.  
183 Analysis were carried out in an Agilent model 1100 series LC coupled to a diode-array  
184 detector set at 306 nm. Data were analysed using Chemstation G2171 v. B.01.03  
185 software (Agilent, USA). The chromatographic system was equipped with a reverse  
186 C18 Alltima column (150 mm x 2.1 mm, particle size 5  $\mu\text{m}$ ; Altech, USA) and a Gemini

187 C18 support AJO-7596 precolumn. The mobile phase, pumped at 0.25 mL/min was a  
188 mixture of water/methanol/acetic acid in a gradient condition. The column was heated  
189 at 40 °C and the injection volume was 10 µL. Under these conditions, the retention time  
190 for resveratrol was 22.8±0.5 min. Calibration curves in ethanol 75% were designed  
191 over the range of 1-100 µg/mL ( $R^2 \geq 0.999$ ). Under these experimental conditions, the  
192 limit of quantitation was calculated to be 200 ng/mL.

193 For analysis, 10 mg nanoparticles were dispersed in 1 mL of water and centrifuged at  
194 30,500 g for 20 min. The amount of encapsulated resveratrol was calculated by  
195 dissolution of the pellets with 1 mL of ethanol 75%. Each sample was assayed in  
196 triplicate and the results were expressed as the amount of resveratrol (µg) per mg of  
197 nanoparticles.

198 The encapsulation efficiency (E.E) was calculated as follows:

199 
$$E. E. (\%) = \frac{Rsv_p}{Rsv_t} \times 100 \quad [\text{Eq. 1}]$$

200 where Rsv-t is the total amount of resveratrol in the formulations and, Rsv-p, the  
201 amount of resveratrol quantified in the pellet.

### 202 **In vitro release study**

203 Release experiments were conducted under sink conditions at 37°C using simulated  
204 gastric (pH 1.2; SGF) and intestinal (pH 6.8; SIF) fluids<sup>22</sup>, containing 0.5% Tween 20  
205 as surfactant to increase the resveratrol aqueous solubility. The studies were  
206 performed under agitation in a slide-A-Lyzer® Dialysis cassette 10000 MWCO (Thermo  
207 scientific, Rockford, IL, USA). For this purpose, the cassette was filled with 3 mg of  
208 resveratrol nanoparticles previously dispersed in 5 mL water and, then, introduced in a  
209 vessel containing 500 mL of SGF (pH 1.2; 37°C) under magnetic stirring. After 2 h in  
210 SGF, the cassette was introduced in another vessel containing 500 mL of thermostat-  
211 zed SIF (pH 6.8; 37°C, under agitation). At different time points, samples were  
212 collected and filtered through 0.45 µm size-pore filters (Thermo scientific, Rockford,

213 USA) before quantification by HPLC. Calibration curves of resveratrol in SGF and SIF  
214 (0.05-6 µg/mL; R2 ≥ 0.999 in both cases) were performed.

215 In order to ascertain the resveratrol release mechanism the obtained data were fitted to  
216 the Korsmeyer-Peppas and the Peppas-Sahlin models. The Korsmeyer–Peppas model  
217 is a simple semi-empirical approach which exponentially relates drug release with the  
218 elapsed time as expressed in the following equation <sup>24</sup>:

$$219 \quad \frac{M_t}{M_\infty} = K_{KP} \cdot t^n \quad [\text{Eq. 2}]$$

220 where  $M_t/M_\infty$  is the drug release fraction at time  $t$ ,  $K_{KP}$  is a constant incorporating the  
221 structural and geometric characteristics of the matrix and  $n$  is the release exponent  
222 indicative of the drug release mechanism <sup>25</sup>. Values close to 0.5 indicate a Case I  
223 (Fickian) diffusion mechanism and values between 0.5 and 0.89 indicate anomalous  
224 (non-Fickian) diffusion. Values of  $n$  between 0.89 and 1 indicate Case II transport,  
225 erosion of the matrix.

226 The contribution of Fickian and non-Fickian release was also evaluated by using the  
227 Peppas–Sahling model equation <sup>26</sup>:

$$228 \quad \frac{M_t}{M_\infty} = K_D \cdot t^{1/2} + K_E \cdot t \quad [\text{Eq. 3}]$$

229 where the first term of the right-hand side is the Fickian contribution ( $K_D$  is the  
230 diffusional constant) and the second term is the Case II erosional contribution ( $K_E$  is the  
231 erosional constant).  $K_D$  and  $K_E$  values were used to calculate the contribution  
232 percentage of diffusion (D) and erosion (E) as follows <sup>26</sup>:

$$233 \quad D = \frac{1}{1 + \frac{K_E t^{0.5}}{K_D}} \quad [\text{Eq 4}]$$

$$234 \quad \frac{E}{D} = \frac{K_E}{K_D} t^{0.5} \quad [\text{Eq 5}]$$

235 Only one portion of the release profile ( $M_t/M_\infty \leq 0.6$ ) was used to fit the experimental  
236 data to the previous equation.

237 **In vivo pharmacokinetic studies in Wistar rats**

238 **Pharmacokinetic studies**

239 Pharmacokinetic studies were performed in male Wistar rats (200-250 g) obtained from  
240 Harlan (Barcelona, Spain). Studies were approved by the Ethical Committee for Animal  
241 Experimentation of the University of Navarra (protocol number 028-11) in accordance  
242 with the European legislation on animal experiments.

243 Prior to the oral administration of the formulations, animals were fasted overnight to  
244 avoid interference with the absorption, allowing free access to water. For the  
245 pharmacokinetic study, rats were randomly divided into 4 groups of 6 animals each.  
246 The three experimental groups were: (i) resveratrol water suspension (Rsv-susp), (ii)  
247 resveratrol solution in a PEG400:water mixture (Rsv-sol) and (iii) resveratrol-loaded  
248 zein nanoparticles (Rsv-NP-Z). As control, a group of animals was treated  
249 intravenously with the PEG400:water (1:1 by vol.) solution of resveratrol. Each animal  
250 received the equivalent amount of resveratrol to a dose of 15 mg/kg body weight either  
251 by oral gavage or intravenously via tail vein.

252 Blood samples were collected at set times after administration (0, 10 min, 30 min, 1 h,  
253 2 h, 4 h, 6 h, 8 h, 24 h and 48 h) in specific plasma tubes (Microvette® 500K3E,  
254 SARSTEDT, Germany). Samples were immediately centrifuged at 9,400 g for 10 min  
255 and plasma aliquots were kept frozen at -80 °C until HPLC analysis of both resveratrol  
256 and resveratrol-3-O-D-glucuronide.

257 **Determination of resveratrol and resveratrol-3-O-D-glucuronide plasma**  
258 **concentration by HPLC**

259 The amount of resveratrol was determined by HPLC-UV following an analytical method  
260 previously reported with minor modifications<sup>27</sup>. Analysis were carried out in an Agilent  
261 model 1100 series LC and diode-array detector set at 306 nm. Data were analysed in a  
262 Chemstation G2171 program (B.01.03). The chromatographic system was equipped  
263 with a reversed-phase C18 Kromasil column (250 mm x 2.1 mm; particle size 5 µm)  
264 and a Gemini C18 support AJO-7596 precolumn. The mobile phase, pumped at 0.5

265 mL/min, was a mixture of water, methanol and acetic acid (50:45:5 by vol.) under  
266 isocratic conditions. The column was thermostated at 30°C and the injection volume  
267 was 30 µL. Under these conditions, the retention times for resveratrol-3-O-D-  
268 glucuronide and resveratrol were  $6.2 \pm 0.5$  min and  $12.6 \pm 0.5$  min, respectively.

269 For analysis, a 100 µL aliquot of plasma was mixed with 50 µL HCl 0.1 N and 500 µL  
270 acetonitrile (for protein precipitation) followed by vigorous shaking. Then, samples were  
271 centrifuged at 4000 rpm for 10 min and the obtained supernatants were evaporated  
272 under vacuum in a Speed Vac® system (Holbrook, NY) at 25°C for 30 min. Finally, 100  
273 µL of a mixture of acetonitrile and water (1:1 by vol.) was added and vigorously stirred  
274 in a vortex for 10 min. Then, and prior to the injection, samples were filtered through  
275 0.45 µm filter (Thermo scientific, Rockford, IL, USA).

276 For quantification, calibration curves were prepared over the range 2 to 70 µg/mL for  
277 the metabolite and 50 to 3,000 ng/mL for resveratrol ( $R^2 \geq 0.99$ ). All the calibration  
278 standards were obtained by adding either resveratrol or resveratrol-3-O-D-glucuronide  
279 in acetonitrile (500 µL) to 100 µL plasma from non-treated animals. Then, the  
280 polyphenol or its metabolite was extracted using the same protocol described above.

281 Under these experimental conditions, the limit of quantification was calculated to be 70  
282 ng/mL, for resveratrol, and 4 µg/mL for the metabolite. Linearity, accuracy and  
283 precision values during the same day (intra-day assay) at low, medium and high  
284 concentrations of both resveratrol and the metabolite were always within the  
285 acceptable limits (relative error and coefficient of variation less than 15%).

#### 286 **Pharmacokinetic data analysis**

287 Resveratrol plasma concentration was plotted against time, and pharmacokinetic  
288 analysis was performed using a non-compartmental model with the WinNonlin 5.2  
289 software (Pharsight Corporation, USA). The following parameters were estimated:  
290 maximal serum concentration ( $C_{max}$ ), time in which  $C_{max}$  is reached ( $T_{max}$ ), area under  
291 the concentration-time curve from time 0 to the last sampling-point (48 h) (AUC), mean  
292 residence time (MRT), clearance (Cl), volume of distribution (V) and half-life in the

293 terminal phase ( $t_{1/2}$ ). Furthermore, the relative bioavailability (Fr %) of resveratrol was  
294 estimated by the following equation:

$$295 \quad Fr (\%) = \frac{AUC_{oral}}{AUC_{iv}} \times 100 \quad (\text{Eq. 6})$$

296 where  $AUC_{i.v.}$  and  $AUC_{oral}$  are the areas under the curve for the iv and oral  
297 administrations, respectively.

### 298 ***In vitro*/*In vivo* correlation (INVIC)**

299 The eventual correlation between *in vitro* and *in vivo* results was conducted by plotting  
300 a point-to-point between the amount of resveratrol released from nanoparticles vs the  
301 fraction of resveratrol absorbed (FRA) calculated from the mean plasma concentration-  
302 time inputs using the Wagner-Nelson equation <sup>28</sup>:

$$303 \quad FRA = \frac{C_t + k \times AUC_{0-t}}{k \times AUC_{0-\infty}} \quad (\text{Eq. 7})$$

304 where  $C_t$  is the plasma concentration of resveratrol at a time  $t$ ,  $k$  is the elimination rate  
305 constant of the polyphenol,  $AUC_{0-t}$  is the area under the resveratrol concentration vs.  
306 time curve from 0 to time  $t$ , and  $AUC_{0-\infty}$  is the area under the curve from 0 to infinity.

307 Linear regression analysis was applied to the *in vitro*–*in vivo* correlation plot and  
308 coefficient of determination ( $R^2$ ) was calculated.

### 309 **Anti-inflammatory efficacy study**

#### 310 **Animal model**

311 Four weeks-old (20-22 g) C57BL/6J female mice were purchased from Harlan  
312 (Barcelona, Spain) and housed in standard animal facilities (6 animals per cage with  
313 free access to food and drinking water). Housing conditions were maintained by  
314 controlled temperature and humidity and with 12 h on/off light cycles. Animals were  
315 allowed to acclimate for one week before the experiment.

316 *In vivo* anti-inflammatory studies were evaluated in an endotoxic shock model set up by  
317 intraperitoneal (ip) administration of LPS at a dose of 40  $\mu$ g per mouse <sup>29</sup>. Before  
318 administration, LPS was dissolved in PBS and vortexed during 30 min to complete  
319 homogenization.

320 On day 1, mice were randomly distributed into four groups. The first group of animals  
321 received an oral dose of 15 mg/kg resveratrol daily as oral solution (Rsv-sol) during 7  
322 days. The second group of animals received the same posology of polyphenol (15  
323 mg/kg resveratrol daily; 7 days) but formulated in zein nanoparticles (Rsv-NP-Z).. As  
324 controls, a group of animals received LPS treatment (positive control group) and  
325 another one received neither LPS nor resveratrol (negative control group).

326 Twenty-four hours after the last dose of resveratrol (day 8) animals were challenged  
327 with 40 µg LPS by ip route. Throughout the study, rectal temperature of mice was  
328 measured until 24 h after challenge. Similarly, animals were observed for any clinical  
329 signs or symptoms of toxicity daily and after the challenge. The severity of symptoms  
330 was scored as follows:: i) (-) absent; ii) (+) weak; iii) (++) moderate; and iv) (+++)   
331 strong. Depending on the activity of animals, their mobility was classified as very low,  
332 low or normal.

333 In addition, 90 min after challenge, blood samples were collected from the retro-orbital  
334 cavity in EDTA-K vials (Microvette® 500K3E, SARSTEDT, Germany), centrifuged at  
335 8,000 g for 10 min for sera collection and stored at -20 °C until use.

#### 336 **Measurement of plasma TNF-α**

337 The concentration of circulating TNF-α in the serum was determined by an enzyme-  
338 linked immunosorbent assay kit (Quantikine® ELISA Mouse TNF-α, MTA00B, R&D  
339 Systems, Minneapolis, USA) according to manufacturer's instructions.

#### 340 **Statistical analysis**

341 Data are expressed as the mean ± standard deviation (S.D.) of at least three  
342 experiments. The non-parametric Kruskal-Wallis followed by Mann-Whitney U-test was  
343 used to investigate statistical differences. In all cases, p< 0.05 was considered to be  
344 statistically significant. All data processing was performed using Graph Pad® Prism  
345 statistical software.

346

#### 347 **Results**

## 348 **Preparation and characterization of nanoparticles**

349 **Table 1** shows the physico-chemical characteristics of the nanoparticles used in this  
350 study. Overall, the mean diameter of empty nanoparticles was smaller than those  
351 loaded with resveratrol. When resveratrol was encapsulated, zein nanoparticles  
352 displayed a mean size of about 310 nm, whereas, the polydispersity index was found to  
353 be lower than 0.2, indicating homogeneous nanoparticle formulations. Furthermore, the  
354 zeta potential of nanoparticles was negative (- 51 mV); however, when resveratrol was  
355 encapsulated the resulting nanoparticles were slightly more negative than for empty  
356 ones (**Table 1**). Additionally, the resveratrol loading was calculated to be about 80  
357  $\mu\text{g}/\text{mg}$  nanoparticles, with an encapsulation efficiency close to 82%.

358 **Figure 1** shows the morphology and shape of resveratrol-loaded nanoparticles. In all  
359 cases, nanoparticles consisted of homogeneous populations of spherical particles with  
360 a smooth surface. In addition, the size of nanoparticles as observed by SEM was in line  
361 with the values determined by photon correlation spectroscopy (**Table 1**).

## 362 **In vitro release profile**

363 **Figure 2A** represents the release profile of resveratrol from nanoparticles expressed  
364 as cumulative percentage of drug released *versus* time. In all cases, the release of  
365 resveratrol from zein-based nanoparticles was found to be independent of the pH  
366 conditions. During the first 2 h, under SGF conditions (pH 1.2), about 20% of the  
367 loaded resveratrol was released from zein nanoparticles. Then, 6 hours later (during  
368 incubation in SIF conditions) the amount released was close to 60% of the total content  
369 of resveratrol. After 48 h, all the loaded resveratrol was released from nanoparticles.

370 The release profile of resveratrol from NPs was fitted to different mathematical release  
371 models. Using the Korsmeyer-Peppas equation,  $R^2$  values were high ( $R^2 > 0.96$ ) and the  
372 exponent “n” value was  $0.75 \pm 0.06$ . All of this suggests that the release of resveratrol  
373 from nanoparticles would be a combination of Fickian diffusion and erosion of the  
374 nanoparticle matrix. Under these circumstances, the Peppas-Sahlin model was applied  
375 and the erosion ( $K_E$ ) and diffusion ( $K_D$ ) constants were calculated ( $K_D = 0.08 \pm 0.02 \text{ h}^{-1/2}$ ;

376  $K_E: 0.04 \pm 0.01 \text{ h}^{-1}$ ). **Figure 2B** displays the contribution of both the diffusion and erosion  
377 mechanisms on the release of resveratrol from zein nanoparticles. The time at which  
378 both mechanisms (diffusion and erosion) contributed in a similar amount to the release  
379 of resveratrol was calculated to be 3.5 h.

### 380 **In vivo pharmacokinetics**

381 **Figure 3A** shows the plasma concentration-time profile of a resveratrol solution in  
382 PEG-400:water (1:1 by vol.) after the intravenous administration to rats of a single dose  
383 of 15 mg/kg. The data were adjusted to a non-compartmental model. The resveratrol  
384 plasma concentration decreased rapidly in a biphasic way during the first 8-h post  
385 administration. The peak plasma concentration ( $C_{max}$ ) of resveratrol was around 15  
386  $\mu\text{g/mL}$ , whereas the AUC and half-life ( $t_{1/2}$ ) were calculated to be 11.4  $\mu\text{g h/mL}$  and 2.0  
387 h, respectively. The resveratrol clearance and its volume of distribution were about 0.2  
388 L/h and 0.6 L, respectively (**Table 2**).

389 **Figure 3B** shows the plasma concentration levels of resveratrol when administered  
390 orally as a single dose of 15 mg/kg to rats. Interestingly, when resveratrol was  
391 formulated as a suspension, no detectable levels of the polyphenol were quantified in  
392 plasma. On the other hand, when resveratrol was administered as solution (Rsv-sol),  
393 the polyphenol plasma levels displayed an initial maximum concentration ( $C_{max}$ ) of  
394 around 0.2  $\mu\text{g/mL}$ , 30 min after administration. Then, the plasma levels of resveratrol  
395 decreased rapidly and quantifiable levels were only detected during the first 4 h post-  
396 administration.

397 For resveratrol-loaded in zein nanoparticles (Rsv-NP-Z), the amount of the polyphenol  
398 in plasma increased during the first 4 h after administration until reaching a maximum.  
399 Then, the resveratrol plasma levels decreased slowly for the following 20 h. Forty-eight  
400 hours post-administration, the amount of resveratrol in plasma was very close to the  
401 quantitation limit of the analytical technique.

402 **Table 2** summarizes the main pharmacokinetic parameters estimated with a non-  
403 compartmental analysis of the experimental data obtained after the administration of

404 the different formulations to rats. The resveratrol AUC values from zein nanoparticle  
405 formulations were significantly higher ( $p < 0.05$ ) than those observed for the polyphenol  
406 solution. Similarly, the resveratrol MRT was thirteen-times higher when administered in  
407 the form of zein nanoparticles than when solubilized in the PEG400:water oral mixture.  
408 Finally, the relative oral bioavailability of resveratrol when incorporated in nanoparticles  
409 was calculated to be 50 % using zein nanoparticles. This value was significantly higher  
410 than the bioavailability obtained with the PEG400:water solution (2.6 %).

411 **Figure 4** shows the plasma concentration *versus* time profile of the resveratrol main  
412 metabolite (resveratrol-O-3-glucuronide) after the single administration of the  
413 polyphenol in the formulations tested. Interestingly, the profile of the plasma curves for  
414 both resveratrol and its metabolite were similar; however, the metabolite levels were  
415 always higher than for the polyphenol. When resveratrol was administered  
416 intravenously, the metabolite concentration reached 41.9  $\mu\text{g/mL}$  ( $C_{\text{max}}$ ) and, then, the  
417 metabolite levels decreased sharply. The AUC value was calculated to be 197  $\mu\text{g}$   
418  $\text{h/mL}$ .

419 For the solution of resveratrol orally administered, the  $C_{\text{max}}$  of the metabolite in plasma  
420 was found to be 2-times lower (22.1  $\mu\text{g/mL}$ ) than when administered by the iv route. In  
421 this case, the metabolite was only quantified in plasma during the first 8 h post-  
422 administration. The AUC value was calculated to be 104  $\mu\text{g h/mL}$ ; around half the i.v.  
423 solution one.

424 For nanoparticles, the metabolite was quantified during the first 24 hours after  
425 administration. In addition, the metabolite AUC data was around 342  $\mu\text{g h/mL}$  for Rsv-  
426 NP-Z. This value was around three-times higher than with the resveratrol was  
427 administered as oral solution or intravenously.

#### 428 **In vitro-in vivo correlations**

429 **Figure 5** represents the relationship between the *in vitro* dissolution data (expressed  
430 as the cumulative percentage of the polyphenol released) and the fraction of

431 resveratrol absorbed during the first 8 h post-administration. An acceptable linear  
432 regression was observed between both data ( $R^2 = 0.83$  for Rsv-NP-Z).

### 433 **Anti-inflammatory efficacy study**

434 **Figure 6A** shows rectal temperature of mice for 24 h after ip administration of 40  $\mu$ g  
435 LPS. Before challenge, all the animals displayed a similar rectal temperature (data not  
436 shown). However, six hours after challenge, important differences were observed  
437 among groups. Thus positive control animals (without any resveratrol treatment)  
438 displayed a body temperature of about 4°C below the basal normal levels. For animals  
439 treated with Rsv-sol the body temperature was 3°C lower than before challenge. On  
440 the contrary, rectal temperature of animals treated with resveratrol loaded in zein  
441 nanoparticles, decreased only 0.5-1 °C. No variations were observed in the control  
442 negative group. Twenty-four hours after challenge animals treated with free resveratrol  
443 or encapsulated regained normal temperature.

444 **Table 3** shows the overall endotoxic symptoms score including the number of animals  
445 displaying a temperature 2 °C lower than the basal temperature, 6 h post-challenge.  
446 Positive control animals displayed a low mobility and signs of bristly hair and  
447 respiratory distress. On the contrary, animals treated with Rsv-NP-Z displayed an  
448 almost normal behaviour and an evident better symptomatology than those animals  
449 receiving resveratrol as oral solution, which appeared to be immobile or with a high  
450 difficulty to coordinate any simple movement.

451 **Figure 6B** shows the serum levels of TNF- $\alpha$  measured by ELISA before and 90 min  
452 after LPS challenge. Negligible levels of TNF- $\alpha$  were observed before LPS  
453 administration. The oral administration of Rsv-NP-Z induced a decrease in the levels of  
454 TNF- $\alpha$  with respect to mice pre-treated with resveratrol solution and the positive control  
455 group; however, these differences were not statistically significant. Significant  
456 differences ( $p < 0.01$ ) were observed between control negative and the rest of groups.

457

### 458 **Discussion**

459 In the past zein was proposed as material for the preparation of nanoparticles due to its  
460 hydrophobic character, degradability, adherence properties and versatile processability  
461 <sup>19,20</sup>. However, as zein possesses abundant non-polar amino acids, the dispersability of  
462 the resulting nanoparticles in an aqueous media (and, therefore, their potential  
463 applications) is a challenge <sup>30</sup>. Recently, the use of citrate and phosphate salts was  
464 proposed to minimize this problem <sup>31</sup>. In our case, lysine was added during the  
465 preparative process of nanoparticles. In this way, the resulting dry powder of zein  
466 nanoparticles was easily redispersed, yielding a homogeneous fine suspension (**Table**  
467 **1**) after the addition of water and simple hand agitation.

468 Resveratrol-loaded zein nanoparticles (Rsv-NP-Z) displayed a mean size close to 300  
469 nm and negative zeta potential. The resveratrol loading was of 80 µg/mg nanoparticles  
470 with an encapsulation efficiency of 80%. This payload is in line with values previously  
471 reported by using solid lipid nanoparticles <sup>17</sup>, PLGA nanoparticles <sup>18</sup>, or nanoemulsions  
472 <sup>32</sup>. The release of resveratrol from zein nanoparticles was found to be pH-independent.  
473 In fact, this phenomenon would be a combination of both Fickian diffusion and erosion  
474 of the nanoparticle matrix (Peppas-Sahlin model). During the first hours of the release  
475 process, resveratrol molecules would mainly diffuse from the nanoparticles to the  
476 aqueous medium by Fickian diffusion. Later (3.5 h), the release of resveratrol would be  
477 mainly due to an erosion and/or relaxation process of the nanoparticle matrix.  
478 Interestingly, as a consequence of both phenomena, the amount of resveratrol  
479 released (at least during the first 8 h) is constant and approaches to a zero order  
480 kinetic.

481 Pharmacokinetic studies were carried out at a single dose of 15 mg/kg, comparable to  
482 those used in previous studies <sup>33,34</sup>. The oral administration of a single dose of  
483 resveratrol as an aqueous suspension (Rsv-susp) to rats did not produce quantifiable  
484 levels of the polyphenol in plasma (**Figure 3B**). For the solution formulation, in a  
485 PEG400:water mixture (Rsv-sol), the plasma levels of the polyphenol were higher than  
486 for the suspension but they rapidly decreased and 6 h-post administration only traces

487 of resveratrol in plasma were detected. These findings are directly related with the  
488 extensive metabolism of resveratrol <sup>35</sup>. In fact, when administered orally, resveratrol  
489 (due to its lipophilic character) can rapidly enter into the enterocyte by passive diffusion  
490 <sup>36</sup>; although, it is highly metabolized to glucuronide and sulphate derivatives, which may  
491 be secreted back to the intestinal lumen through multidrug resistance protein 2 (MRP2)  
492 and BCRP <sup>37,38</sup>. This extensive biotransformation of resveratrol decreases circulation  
493 levels of free resveratrol and facilitates its excretion (in the form of conjugates) by the  
494 kidneys via urine <sup>14</sup>. Controversy remains about the physiological activity of metabolites  
495 or if they can act as resveratrol prodrugs. There are evidences that, at sufficient  
496 concentrations, resveratrol metabolites have biological activity in various tissues <sup>36</sup>.  
497 Nevertheless, there are also evidences that these compounds have no effects in some  
498 tissues <sup>39</sup>.

499 However, when resveratrol was administered after its encapsulation in zein  
500 nanoparticles, sustained and prolonged plasma levels of the polyphenol were observed  
501 for at least 24 h (**Figure 3B**) and its relative oral bioavailability was about 50% (**Table**  
502 **3**), which is about 18-fold higher than the value observed for Rsv-sol (about 2.6%). This  
503 increased capability to promote the absorption and bioavailability of resveratrol by  
504 using zein nanoparticles would be related with its high hydrophobic character, that  
505 would offer a higher stability *in vivo*, and to the capability of this corn protein to develop  
506 mucoadhesive interactions within the gut mucus layer <sup>40</sup>. Thus, this characteristic would  
507 provide a longer residence in close contact with the intestinal epithelium and facilitating  
508 the establishment of a concentration gradient from the nanoparticulate matrix untill the  
509 absorptive membrane. Interestingly, the fraction of resveratrol absorbed from zein  
510 nanoparticles correlated well with the percentage of the polyphenol released *in vitro*  
511 (see **Figure 5**).

512 In previous studies, it has been reported that the oral bioavailability of resveratrol is  
513 almost zero <sup>34,41</sup>. In order to improve its absorption different strategies have been  
514 proposed such as the use of oral absorption enhancers (e.g. Tween 80, cyclodextrins)

515 or the employment of resveratrol derivatives. In this way, Kapetanovic and co-workers  
516 have reported an oral bioavailability of resveratrol (formulated as aqueous solution  
517 containing methylcellulose and Tween 80) close to 30% after the administration of a  
518 single dose of 50 mg/kg in rats. In the same work, the administration of the same  
519 resveratrol formulation at a dose of 150 mg/kg produced an oral bioavailability of 19%  
520 <sup>42</sup>. In another work, resveratrol trimethyl-ether administered orally in a solution  
521 formulated with randomly methylated- $\beta$ -cyclodextrin (15 mg/kg) yielded a bioavailability  
522 of about 47%. More recently, the use of nanocarriers has also been proposed. Thus, in  
523 mice and using a dose of 50 mg/kg, the oral bioavailability of resveratrol when loaded  
524 in either Eudragit or chitosan/lecithin nanoparticles was calculated to be 39 and 61%,  
525 respectively <sup>43</sup>. For solid lipid nanoparticles, the oral bioavailability of the polyphenol  
526 was found to be 8-fold higher than for a conventional solution of resveratrol <sup>44</sup>. In our  
527 case, the resveratrol bioavailability was 18-fold higher when loaded in zein  
528 nanoparticles than when dissolved in the PEG400:water solution. Furthermore, zein  
529 nanoparticles offering sustained and prolonged levels of resveratrol in plasma provided  
530 a supplementary advantage when compared with other strategies.

531 Regarding the presence of the main metabolite (resveratrol-O-3-glucuronide <sup>13</sup>) in the  
532 plasma of animals, the levels of this compound (measured as AUC) were higher when  
533 resveratrol was administered encapsulated in zein nanoparticles than when  
534 administered in the conventional solution both by iv route (about 1.7 times) or orally  
535 (around 3.3 times). This fact would be related with the slow release of the polyphenol  
536 from the nanoparticles (where protected from degradation) and a prolonged residence  
537 of nanoparticles in the gut mucosa due to their mucoadhesive properties. In other  
538 words, by using nanoparticles, more resveratrol and during a longer period would reach  
539 the circulation, counterbalancing the natural rapid metabolism of the drug.

540 Finally, we studied the anti-inflammatory activity of resveratrol when loaded in zein  
541 nanoparticles. Several *in vitro* and *in vivo* studies suggest that resveratrol inhibits the  
542 inflammatory response mediated by microbial stimuli <sup>45</sup>; by inhibiting the transcription

543 factor NF- $\kappa$ B<sup>10,11</sup>. Therefore, we tested here the protective effect of encapsulated  
544 resveratrol against the inoculation of LPS in mice. LPS is present exclusively on the  
545 outer membrane of Gram negative bacteria, and consequently, it is one of the most  
546 strong alarm signals for the innate immune system, inducing in animals a  
547 pathophysiologic syndrome known as endotoxic shock. This syndrome is similar to  
548 sepsis shock syndrome that progress on multiple organ failure<sup>29,46</sup>, showing  
549 piloerection, hypothermia, shivering, tachycardia and lethargy. These symptoms are  
550 related with large amounts of released inflammatory mediators, such as TNF- $\alpha$ , NO  
551 and prostaglandin E2 (PGE2), where TNF- $\alpha$  play a central role as being the first one to  
552 be released<sup>10</sup>. In our experimental conditions, untreated mice challenged with LPS  
553 (positive control) displayed the highest decrease in rectal temperature and the highest  
554 TNF- $\alpha$  serum level. In contrast, Rsv-NP-Z administered daily during 7 days, were able  
555 to diminish endotoxic symptoms like hypothermia or piloerection and increase the  
556 movement of mice compared to those treated with resveratrol solution on daily basics  
557 (**Figure 6, Table 3**). Moreover, for animals treated with Rsv-NP-Z, TNF- $\alpha$  levels were  
558 lower than for controls; although the high variability of values abolished the statistical  
559 significance. These results appear to indicate that the presence of sustained high  
560 levels of resveratrol in plasma could be efficient to reduce the inflammatory mediators  
561 in endotoxic shock induced by LPS.

562 In summary, zein nanoparticles appear to be interesting carriers for the oral delivery of  
563 resveratrol. The polyphenol is released from this carrier by a combination of both  
564 diffusion and erosion of the nanoparticle matrix, providing higher and more prolonged  
565 plasma levels of resveratrol up to 48 h. Consequently, these nanocarriers significantly  
566 increased the oral bioavailability of resveratrol reaching a value close to 50%. The oral  
567 administration of these nanoparticles during one week to mice challenged with LPS  
568 protected them from the inflammatory symptoms and mediators of the endotoxic shock.  
569 Future studies should be performed to ascertain how this treatment modulates TNF- $\alpha$

570 production in order to explore the potential use of Rsv-NP-Z as anti-inflammatory  
571 treatment.

572

### 573 **Acknowledgements**

574 This work was supported by the Regional Government of Navarra (Alimentos  
575 funcionales, Euroinnova call) and the Spanish Ministry of Science and Innovation and  
576 Gobierno de Navarra (ADICAP; ref. IPT-2011-1717-900000). Rebeca Penalva  
577 acknowledges the “Asociación de Amigos Universidad de Navarra” for the financial  
578 support.

579

580 **References**

- 581 1. Baur, J.A.; Sinclair, D.A. Therapeutic potential of resveratrol: the in vivo evidence. *Nat Rev*  
582 *Drug Discov.* **2006**, *5*, 493-506.
- 583 2. Amri, A.; Chaumeil, J.C.; Sfar, S.; Charrueau, C. Administration of resveratrol: What  
584 formulation solutions to bioavailability limitations? *J. Control. Release* **2012**, *158*, 182-193.
- 585 3. Kasiotis, K.M.; Pratsinis, H.; Kletsas, D.; Haroutounian, S.A. Resveratrol and related  
586 stilbenes: Their anti-aging and anti-angiogenic properties. *Food Chem. Toxicol.* **2013**, *61*, 112-  
587 120.
- 588 4. Orallo, F.; Alvarez, E.; Camina, M.; Leiro, J.M.; Gomez, E.; Fernandez, P. The possible  
589 implication of trans-Resveratrol in the cardioprotective effects of long-term moderate wine  
590 consumption. *Mol. Pharmacol.* **2002**, *61*, 294-302.
- 591 5. Li, S.; Wang, X.; Kong, L. Design, synthesis and biological evaluation of imine resveratrol  
592 derivatives as multi-targeted agents against Alzheimer's disease. *Eur. J. Med. Chem.* **2014**, *71*,  
593 36-45.  
594
- 595 6. Singh, G.; Pai, R.S. Recent advances of resveratrol in nanostructured based delivery  
596 systems and in the management of HIV/AIDS. *J. Control. Release.* **2014**, *194*, 178–188.
- 597 7. Palsamy, P.; Subramanian, S. Resveratrol protects diabetic kidney by attenuating  
598 hyperglycemia-mediated oxidative stress and renal inflammatory cytokines via Nrf2–Keap1  
599 signaling. *Biochim. Biophys. Acta.* **2011**, *1812*, 719-731.
- 600 8. Timmers, S.; Konings, E.; Bilet, L.; Houtkooper, R.H.; van de Weijer, T.; Goossens, G.H.;  
601 Hoeks, J.; van der Krieken, S.; Ryu, D.; Kersten, S. Calorie restriction-like effects of 30 days of  
602 resveratrol supplementation on energy metabolism and metabolic profile in obese humans. *Cell*  
603 *Metab.* **2011**, *14*, 612-622.
- 604 9. Gillum, M.P.; Kotas, M.E.; Erion, D.M.; Kursawe, R.; Chatterjee, P.; Nead, K.T.; Muise, E.S.;  
605 Hsiao, J.J.; Frederick, D.W.; Yonemitsu, S.; Banks, A.S.; Qiang, L.; Bhanot, S.; Olefsky, J.M.;  
606 Sears, D.D.; Caprio, S.; Shulman, G.I. SirT1 regulates adipose tissue inflammation. *Diabetes*  
607 **2011**, *60*, 3235-3245.
- 608 10. Farghali, H.; Černý, D.; Kameníková, L.; Martínek, J.; Hořínek, A.; Kmoníčková, E.; Zídek, Z.  
609 Resveratrol attenuates lipopolysaccharide-induced hepatitis in D-galactosamine sensitized rats:  
610 role of nitric oxide synthase 2 and heme oxygenase-1. *Nitric Oxide.* **2009**, *21*, 216-225.
- 611 11. de la Lastra, C.A.; Villegas, I. Resveratrol as an anti-inflammatory and anti-aging agent:  
612 Mechanisms and clinical implications. *Mol. Nutr. Food Res.* **2005**, *49*, 405-430.
- 613 12. Walle, T. Absorption and metabolism of flavonoids. *Free Radic. Biol. Med.* **2004**, *36*, 829-  
614 837.
- 615 13. Kuhnle, G.; Spencer, J.P.; Chowrimootoo, G.; Schroeter, H.; Debnam, E.S.; Srai, S.K.S.;  
616 Rice-Evans, C.; Hahn, U. Resveratrol is absorbed in the small intestine as resveratrol  
617 glucuronide. *Biochem. Biophys. Res. Commun.* **2000**, *272*, 212-217.
- 618 14. Walle, T.; Hsieh, F.; DeLegge, M.H.; Oatis, J.E., Jr; Walle, U.K. High absorption but very low  
619 bioavailability of oral resveratrol in humans. *Drug Metab. Dispos.* **2004**, *32*, 1377-1382.
- 620 15. Planas, J.M.; Alfaras, I.; Colom, H.; Juan, M.E. The bioavailability and distribution of  
621 trans-resveratrol are constrained by ABC transporters. *Arch. Biochem. Biophys.* **2012**, *527*, 67-  
622 73.

- 623 16. Bolko, K.; Zvonar, A.; Gašperlin, M. Mixed lipid phase SMEDDS as an innovative approach  
624 to enhance resveratrol solubility. *Drug Dev. Ind. Pharm.* **2013**, *40*, 102-109.
- 625 17. Teskač, K.; Kristl, J. The evidence for solid lipid nanoparticles mediated cell uptake of  
626 resveratrol. *Int. J. Pharm.* **2010**, *390*, 61-69.
- 627 18. Singh, G.; Pai, R.S. Optimized PLGA nanoparticle platform for orally dosed trans-resveratrol  
628 with enhanced bioavailability potential. *Expert Opin. Drug Del.* **2014**, *11*, 647-659.
- 629 19. Anderson, T.J.; Lamsal, B.P. Zein extraction from corn, corn products, and coproducts and  
630 modifications for various applications: A review. *Cereal Chem.* **2011**, *88*, 159-173.
- 631 20. Paliwal, R.; Palakurthi, S. Zein in controlled drug delivery and tissue engineering. *J. Control.*  
632 *Release* **2014**, *189*, 108-122.
- 633 21. Shi, K.; Kokini, J.L.; Huang, Q. Engineering zein films with controlled surface morphology  
634 and hydrophilicity. *J. Agric. Food Chem.* **2009**, *57*, 2186–2192
- 635 22. Penalva, R.; Esparza, I.; Agüeros, M.; Gonzalez-Navarro, C.J.; Gonzalez-Ferrero, C.;  
636 Irache, J.M. Casein nanoparticles as carriers for the oral delivery of folic acid. *Food Hydrocol.*  
637 **2015**, *44*, 399–406.
- 638 23. Iacopini, P.; Baldi, M.; Storchi, P.; Sebastiani, L. Catechin, epicatechin, quercetin, rutin and  
639 resveratrol in red grape: content, in vitro antioxidant activity and interactions. *J. Food Comp.*  
640 *Anal.* **2008**, *21*, 589-598.
- 641 24. Ritger, P.L.; Peppas, N.A. A simple equation for description of solute release I. Fickian and  
642 non-Fickian release from non-swellable devices in the form of slabs, spheres, cylinders or discs.  
643 *J. Control. Release* **1987**, *5*, 23-36.
- 644 25. Sujja-areevath, J.; Munday, D.L.; Cox, P.J.; Khan, K.A. Relationship between swelling,  
645 erosion and drug release in hydrophilic natural gum mini-matrix formulations. *Eur. J. Pharm.*  
646 *Sci.* **1998**, *6*, 207-217.
- 647 26. Peppas, N.A.; Sahlin, J.J. A simple equation for the description of solute release. III.  
648 Coupling of diffusion and relaxation. *Int. J. Pharm.* **1989**, *57*, 169-172.
- 649 27. Boocock, D.J.; Patel, K.R.; Faust, G.E.S.; Normolle, D.P.; Marczylo, T.H.; Crowell, J.A.;  
650 Brenner, D.E.; Booth, T.D.; Gescher, A.; Steward, W.P. Quantitation of trans-resveratrol and  
651 detection of its metabolites in human plasma and urine by high performance liquid  
652 chromatography. *J Chromatogr B Analyt Technol Biomed Life Sci.* **2007**, *848*, 182-187.
- 653 28. Kassem, M.A.; ElMeshad, A.N.; Fares, A.R. Enhanced bioavailability of buspirone  
654 hydrochloride via cup and core buccal tablets: Formulation and in vitro/in vivo evaluation. *Int. J.*  
655 *Pharm.* **2014**, *463*, 68-80.
- 656 29. Nemzek, J.A.; Hugunin, K.M.S.; Opp, M.R. Modeling sepsis in the laboratory: merging sound  
657 science with animal well-being. *Comp. Med.* **2008**, *58*, 120–128.
- 658 30. Chen, H.; Zhong, Q. Processes improving the dispersibility of spray-dried zein nanoparticles  
659 using sodium caseinate. *Food Hydrocoll.* **2014**, *35*, 358-366.
- 660 31 Molina, M.I.; Wagner, J.R. The effects of divalent cations in the presence of phosphate,  
661 citrate and chloride on the aggregation of soy protein isolate. *Food Res. Int.* **1999**, *32*, 135-143.

- 662 32. Sessa, M.; Balestrieri, M.L.; Ferrari, G.; Servillo, L.; Castaldo, D.; D'Onofrio, N.; Donsì, F.;  
663 Tsao, R. Bioavailability of encapsulated resveratrol into nanoemulsion-based delivery systems.  
664 *Food Chem.* **2014**, *147*, 42-50.
- 665 33. Colom, H.; Alfaras, I.; Maijó, M.; Juan, M.E.; Planas, J.M. Population pharmacokinetic  
666 modeling of trans-resveratrol and its glucuronide and sulfate conjugates after oral and  
667 intravenous administration in rats. *Pharm. Res.* **2011**, *28*, 1606-1621.
- 668 34. Lin, H.S.; Ho, P.C., Preclinical pharmacokinetic evaluation of resveratrol trimethyl ether in  
669 Sprague-Dawley rats: the impacts of aqueous solubility, dose escalation, food and repeated  
670 dosing on oral bioavailability. *J Pharm. Sci.* **2011**, *100*, 4491-4500.
- 671 35. Wenzel, E.; Soldo, T.; Erbersdobler, H.; Somoza, V. Bioactivity and metabolism of trans-  
672 resveratrol orally administered to Wistar rats. *Mol. Nutr. Food Res.* **2005**, *49*, 482-494.
- 673 36. Smoliga, M.; Blanchard, O. Enhancing the delivery of resveratrol in humans: If low  
674 bioavailability is the problem, what is the solution? *Molecules* **2014**, *19*, 17154-17172.
- 675 37. Juan, M.E.; Gonzalez-Pons, E.; Planas, J.M. Multidrug Resistance Proteins Restrain the  
676 Intestinal Absorption of trans-Resveratrol in Rats. *J. Nutr.* **2010**, *140*, 489-495.
- 677 38. Alfaras, I.; Pérez, M.; Juan, M.E.; Merino, G.; Prieto, J.G.; Planas, J.M.; Alvarez,, A.I.  
678 Involvement of breast cancer resistance protein (BCRP1/ABCG2) in the bioavailability and  
679 tissue distribution of trans-resveratrol in knockout mice. *J. Agric. Food Chem.* **2010**, *58*, 4523-  
680 4528.
- 681 39. Kenealey, J.D.; Subramanian, L.; van Ginkel, P.R.; Darjatmoko, S.; Lindstrom, M.J.;  
682 Somoza, V.; Ghosh, S.K.; Song, Z.; Hsung, R.P.; Kwon, G.S.; Eliceiri, K.W.; Albert, D.M.;  
683 Polans, A.S. Resveratrol metabolites do not elicit early pro-apoptotic mechanisms in  
684 neuroblastoma cells. *J. Agric. Food Chem.* **2011**, *59*, 4979-4986.
- 685 40. Yin, Y.; Yin, S.; Yang, X.; Tang, C.; Wen, S.; Chen, Z.; Xiao, B.; Wu, L. Surface modification  
686 of sodium caseinate films by zein coatings. *Food Hydrocoll.* **2014**, *36*, 1-8.
- 687 41. Wenzel, E.; Somoza, V. Metabolism and bioavailability of trans-resveratrol. *Mol. Nutr. Food*  
688 *Res.* **2005**, *49*, 472-481.
- 689 42. Kapetanovic, I.M.; Muzzio, M.; Huang, Z.; Thompson, T.N.; McCormick, D.L..  
690 Pharmacokinetics, oral bioavailability, and metabolic profile of resveratrol and its dimethylether  
691 analog, pterostilbene, in rats. *Cancer Chemother. Pharmacol.* **2011**, *68*, 593-601.
- 692 43. Oganessian, E.; Miroshnichenko, I.; Vikhrieva, N.; Lyashenko, A.; Leshkov, S.Y. Use of  
693 nanoparticles to increase the systemic bioavailability of trans-resveratrol. *Pharm. Chem. J.*  
694 **2010**, *44*, 74-76.
- 695 44. Pandita, D.; Kumar, S.; Poonia, N.; Lather, V. Solid lipid nanoparticles enhance oral  
696 bioavailability of resveratrol, a natural polyphenol. *Food Res. Int.* **2014**, *62*, 1165-1174.
- 697 45. Youn, H.S.; Lee, J.Y.; Fitzgerald, K.A.; Young, H.A.; Akira, S.; Hwang, D.H. Specific  
698 inhibition of MyD88-independent signaling pathways of TLR3 and TLR4 by resveratrol:  
699 molecular targets are TBK1 and RIP1 in TRIF complex. *J. Immunol.* **2005**, *175*, 3339-3346.
- 700 46. Yang, Y.; Li, S.; Yang, Q.; Shi, Y.; Zheng, M.; Liu, Y.; Chen, F.; Song, G.; Xu, H.; Wan, T.;  
701 He, J.; Chen, Z. Resveratrol reduces the proinflammatory effects and lipopolysaccharide-  
702 induced expression of HMGB1 and TLR4 in RAW264.7 cells. *Cell Physiol Biochem.* **2014**, *33*,  
703 1283-1292



705 **Figure captions**

706 **Figure 1.** Scanning electron microscopy (SEM) microphotograph of resveratrol-loaded  
707 zein nanoparticles. Bar indicates the resolution (1  $\mu\text{m}$ ). The white box delimits a  
708 magnified area.

709 **Figure 2.** Resveratrol release from zein-based nanoparticles (Rsv-NP-Z). A)  
710 Resveratrol release profile when incubated in simulated gastric (SGF, pH 1.2; 0-2 h)  
711 and simulated intestinal fluids (SIF, pH 6.8; 2-48 h) under sink conditions. Data  
712 represented as mean  $\pm$  SD (n=3). B) Fraction contribution of the Fickian diffusion ( $\bullet$ )  
713 and the erosion/relaxation ( $\circ$ ) mechanisms to resveratrol release from zein  
714 nanoparticles (Rsv-NP-Z).

715 **Figure 3.** Resveratrol plasma concentration vs time after a single administration of the  
716 polyphenol at a dose of 15 mg/kg. A) Intravenous administration of the resveratrol  
717 solution in the PEG400:water mixture. B) Oral administration of the following  
718 resveratrol formulations: i) resveratrol suspension (Rsv-susp,  $\blacktriangle$ ), ii) resveratrol solution  
719 (Rsv-Sol,  $\blacklozenge$ ) and iii) resveratrol-loaded zein nanoparticles (Rsv-NP-Z,  $\blacksquare$ ). Data  
720 expressed as mean  $\pm$  SD (n=6).

721 **Figure 4.** Resveratrol-O-3-glucuronide concentration vs time after a single  
722 administration (intravenous or oral) of the different formulations at dose of 15 mg/kg. i)  
723 Resveratrol intravenous (Rsv-IV,  $\diamond$ ) ii) Oral resveratrol solution (Rsv-Sol,  $\blacktriangle$ ), and iii)  
724 Oral resveratrol loaded in zein nanoparticles (Rsv-NP-Z,  $\blacksquare$ ). Data expressed as mean  $\pm$   
725 SD, n= 6.

726 **Figure 5.** Relationship between fractions dissolved in vitro vs. fraction absorbed in vivo  
727 of Resveratrol loaded into zein nanoparticles (Rsv-NP-Z). FRD (fraction of resveratrol  
728 dissolved), FRA (fraction of resveratrol absorbed).

729 **Figure 6:** Anti-inflammatory activity of resveratrol. A) Comparative of decreased rectal  
730 temperature of mouse after ip administration of LPS (40 µg) on time. B) TNF-α serum  
731 levels before and 1.5 h post LPS (40 µg) administration. Mice were pre-treated orally  
732 daily for 7 days with resveratrol loaded in zein nanoparticles (Rsv-NP-Z) or resveratrol  
733 solubilized in PEG400-H<sub>2</sub>O (Rsv-sol) (1:1 by vol.). No pre-treated with resveratrol  
734 (control +) and negative controls (no pretreated with resveratrol and no treated with  
735 LPS) were also included. Results expressed as mean ± SD (n=6).\*\*\*p<0.01 Kruskal  
736 Wallis test.

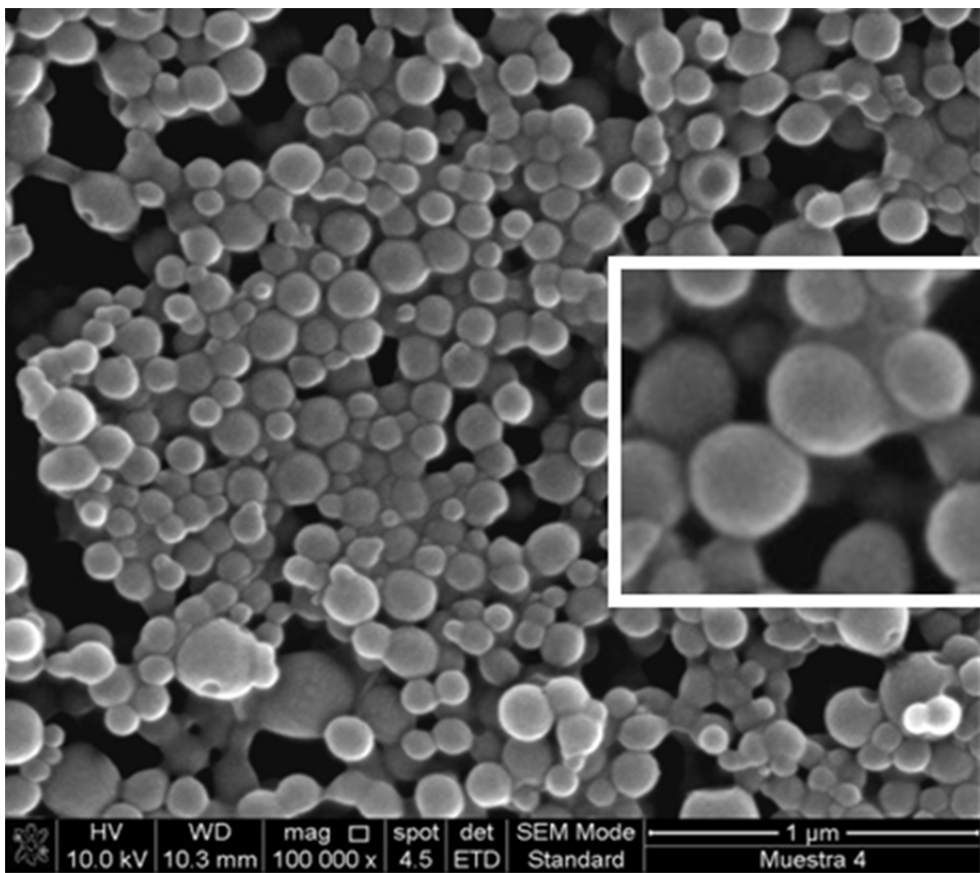


Figure 1.

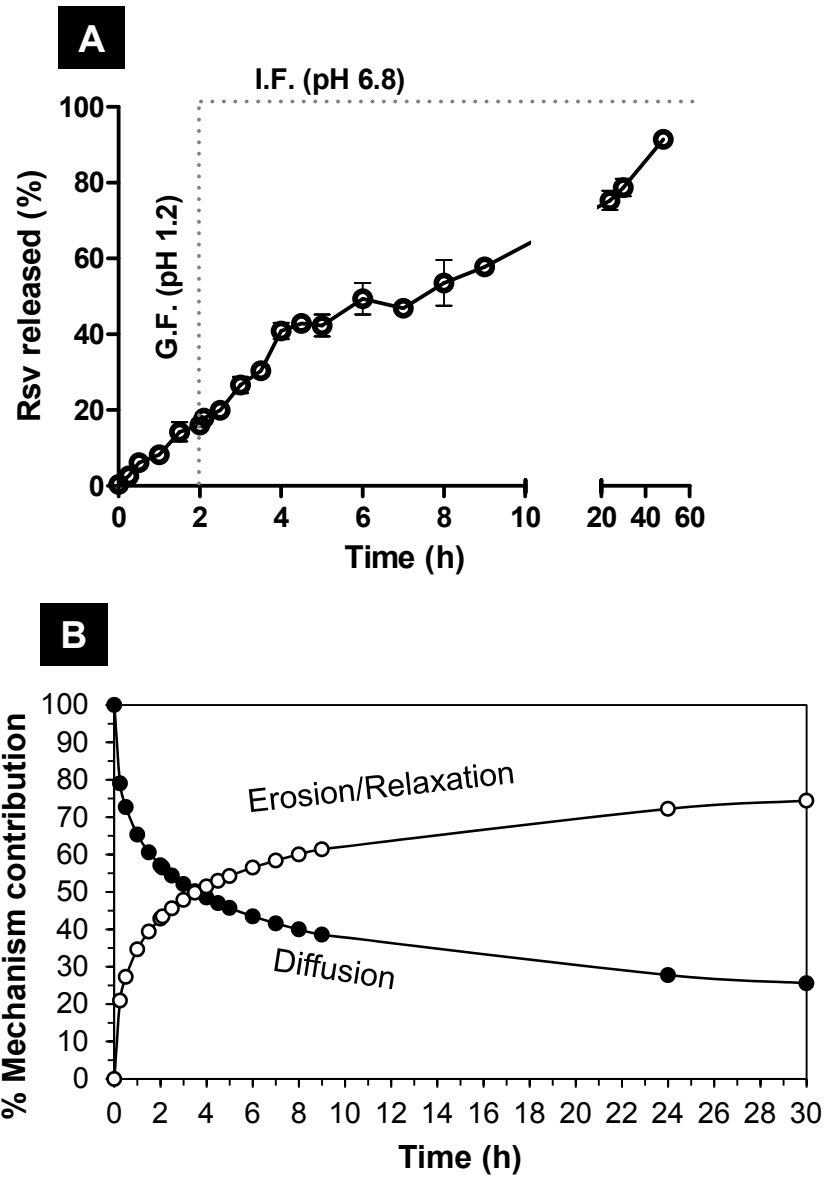


Figure 2.

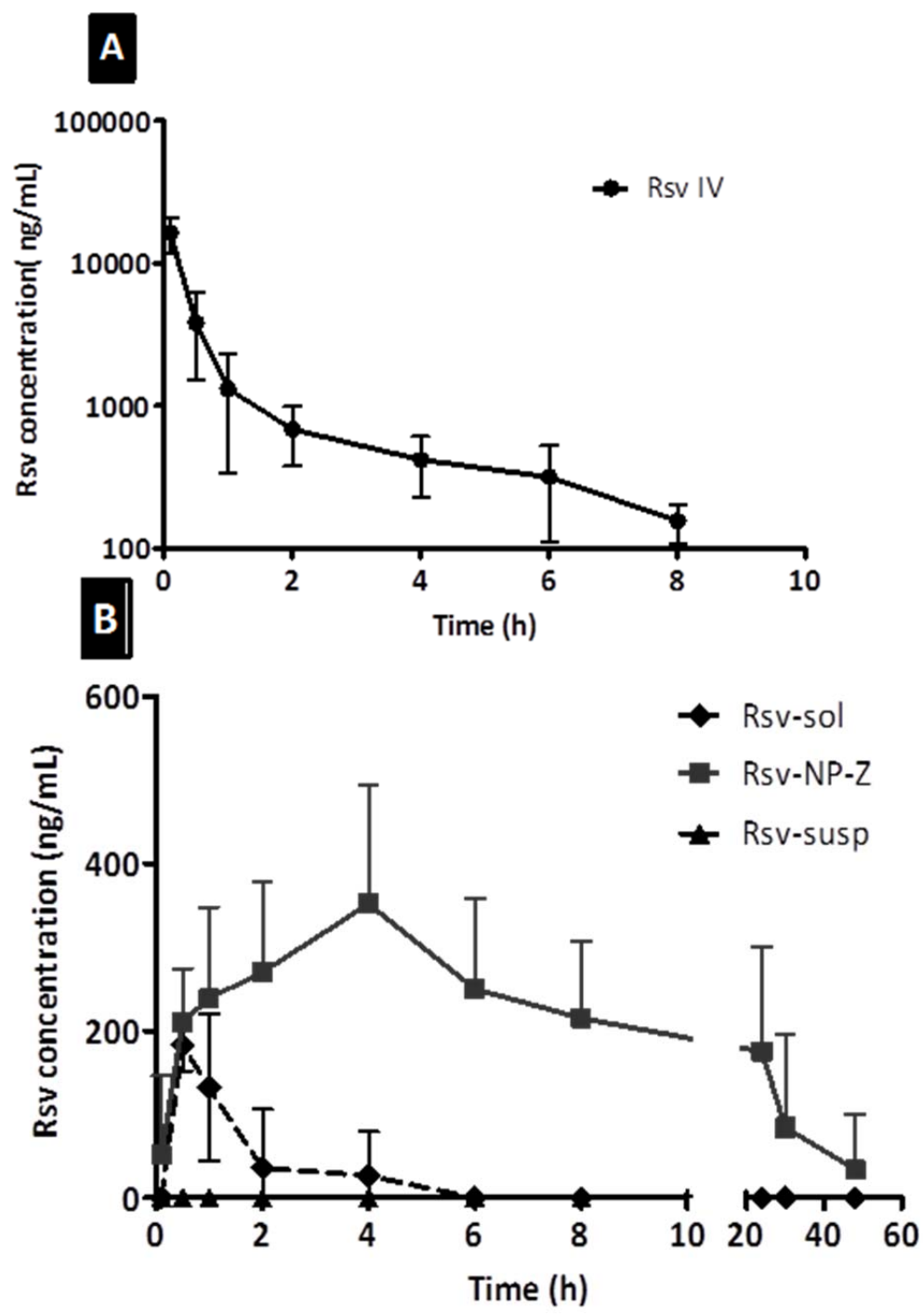


Figure 3.

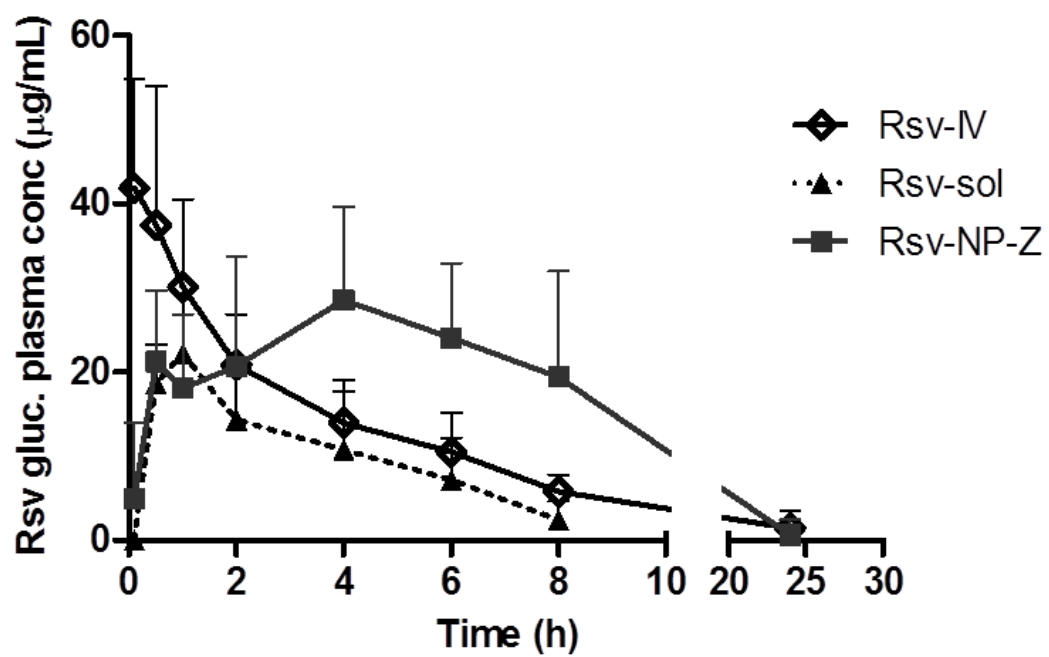


Figure 4.

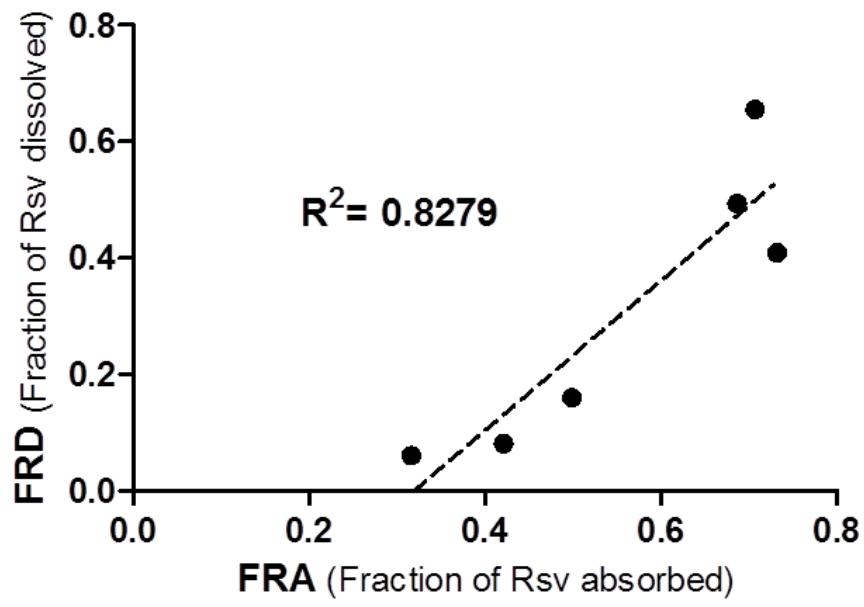


Figure 5.

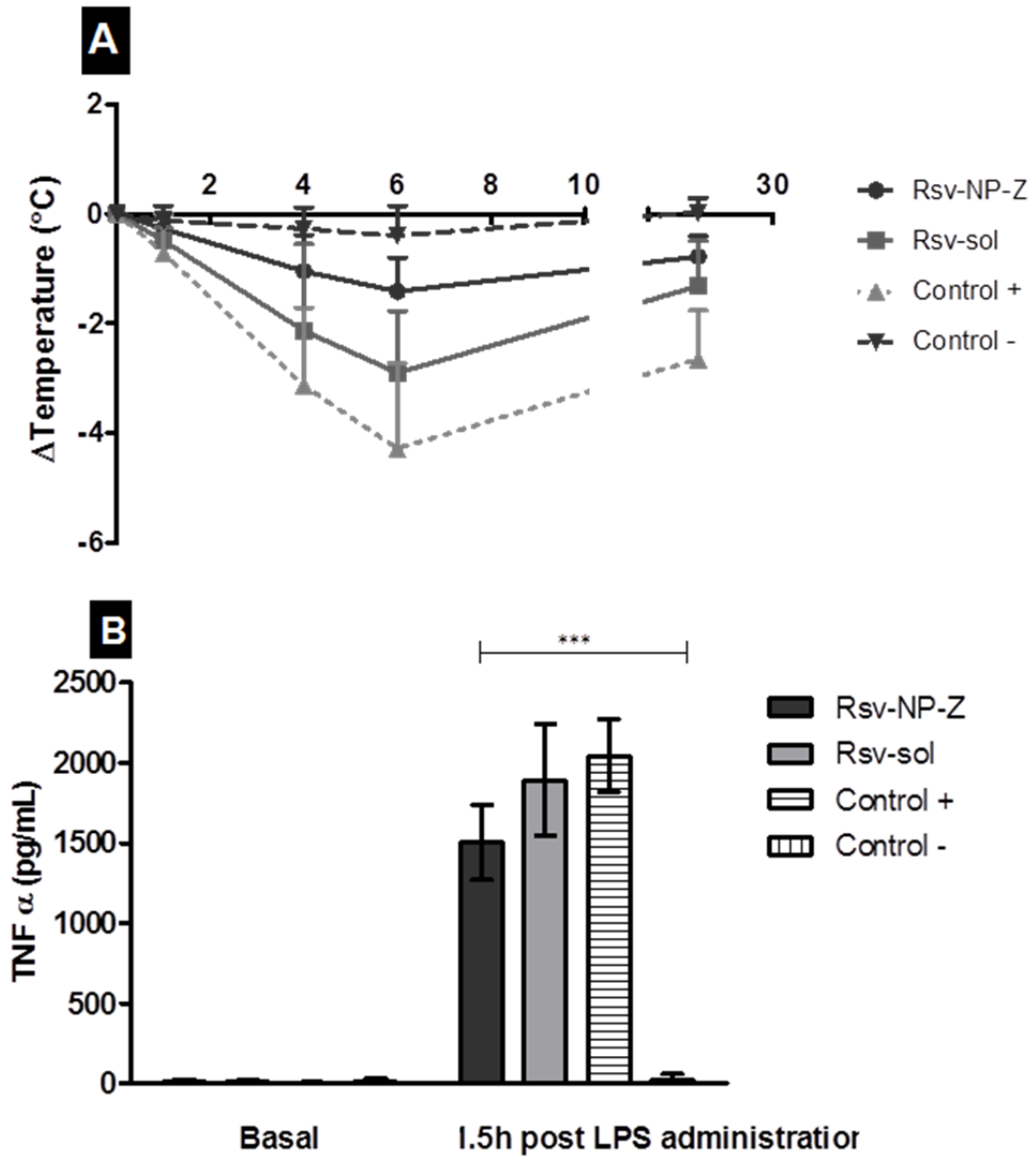


Figure 6.

## Tables

**Table 1.** Physico-chemical characteristics of empty and resveratrol-loaded nanoparticles. NP-Z: empty zein nanoparticles; Rsv-NP-Z: resveratrol-loaded zein nanoparticles. PDI: polydispersity index. Data expressed as mean  $\pm$  SD, n=6.

|                 | Size<br>(nm) <sup>a</sup> | PDI             | Zeta potential<br>(mV) | Rsv loading<br>( $\mu$ g/mg NP) <sup>b</sup> | E.E.<br>(%) <sup>c</sup> |
|-----------------|---------------------------|-----------------|------------------------|--|--------------------------|
| <b>NP-Z</b>     | 264 $\pm$ 2               | 0.07 $\pm$ 0.01 | -46 $\pm$ 2            |  |                          |
| <b>Rsv-NP-Z</b> | 307 $\pm$ 3               | 0.10 $\pm$ 0.01 | -51 $\pm$ 0            | 80 $\pm$ 3                                   | 82 $\pm$ 4               |

<sup>a</sup> Determination of volume mean diameter by photon correlation spectroscopy

<sup>b</sup> Determination of resveratrol content by HPLC-UV

<sup>c</sup> Encapsulation efficiency (%)

**Table 2.** Pharmacokinetic parameters of resveratrol obtained after the administration of the different formulations tested at a dose of 15 mg/kg to Wistar male rats. i) Resveratrol intravenous (Rsv-iv) ii) Rsv solution (Rsv-sol), iii) Resveratrol suspension (Rsv-susp) and iv) Resveratrol loaded in zein nanoparticles (Rsv-NP-Z). Data expressed as mean  $\pm$  SD. (n=6)

|                 | Route | C <sub>max</sub><br>( $\mu$ g/mL) | T <sub>max</sub><br>(h) | AUC<br>( $\mu$ g h/mL)       | T <sub>1/2</sub><br>(h) | Cl<br>(mL/h)   | Vd<br>(mL)    | MRT<br>(h)                   | Fr<br>(%) |
|-----------------|-------|-----------------------------------|-------------------------|------------------------------|-------------------------|----------------|---------------|------------------------------|-----------|
| <b>Rsv iv.</b>  | iv    | 15.2 $\pm$ 5.18                   | 0.1 $\pm$ 0.0           | 10.4 $\pm$ 3.80              | 2.0 $\pm$ 0.5           | 199 $\pm$ 89.8 | 569 $\pm$ 221 | 2.4 $\pm$ 1.0                | 100       |
| <b>Rsv-sol</b>  | oral  | 0.20 $\pm$ 0.02*                  | 0.6 $\pm$ 0.2           | 0.28 $\pm$ 0.13*             | 0.3 $\pm$ 0.2           | 387 $\pm$ 225  | 112 $\pm$ 104 | 1.3 $\pm$ 0.8                | 2.6       |
| <b>Rsv-susp</b> | oral  | ND                                | ND                      | ND                           | ND                      | ND             | ND            | ND                           | ND        |
| <b>Rsv-NP-Z</b> | oral  | 0.39 $\pm$ 0.11 <sup>††</sup>     | 4.9 $\pm$ 3.1           | 5.17 $\pm$ 2.61 <sup>†</sup> | 5.5 $\pm$ 1.7           | 125 $\pm$ 41   | 909 $\pm$ 184 | 17.1 $\pm$ 7.1 <sup>††</sup> | 50.0      |

C<sub>max</sub>: peak plasma concentration; T<sub>max</sub>: time to reach plasma concentration; AUC: Area under the curve; t<sub>1/2</sub>: half life of the terminal phase; Cl: Clearance; MRT: mean residence time Fr: relative oral bioavailability

<sup>†</sup> Significant differences vs Rsv-Sol (p<0.05) Mann-Whitney-U

\* Significant differences vs Rsv-i.v. (p<0.01) Mann-Whitney-U

**Table 3.** Endotoxic symptoms in the resveratrol treated vs no treated LPS-inoculated mice.

| <b>Treatment*</b> | <b>T<sup>a</sup> decreased**<br/>&gt;2°C</b> | <b>Piloerection</b> | <b>Mobility</b> |
|-------------------|--|---------------------|-----------------|
| <b>Control -</b>  | 0/6  | -                   | Normal          |
| <b>Control +</b>  | 6/6  | +++                 | Very low        |
| <b>Rsv-Sol</b>    | 4/6  | ++                  | Very Low        |
| <b>Rsv-NP-Z</b>   | 1/6  | +                   | Low             |

\*Control -: No treated, no LPS; Control +: No treated but inoculated with LPS; Rsv-Sol: administration of resveratrol solution daily during 7 days, LPS; Rsv-NP-Z: administration of resveratrol-loaded zein nanoparticles daily during 7 days, LPS. (n=6). Severity of the symptoms: (-) None; (+) weak; (++) moderate; (+++) strong.

\*\* , Decreased of temperature 6 h after LPS inoculation.

# TOC Graphic

